View Journal

NJC

New Journal of Chemistry

A journal for new directions in chemistry

Accepted Manuscript

This article can be cited before page numbers have been issued, to do this please use: A. Q. Ramle, E. R. T. Tiekink, C. F. Chee, N. Muhd Julkapli and W. J. Basirun, *New J. Chem.*, 2020, DOI: 10.1039/D0NJ04357E.

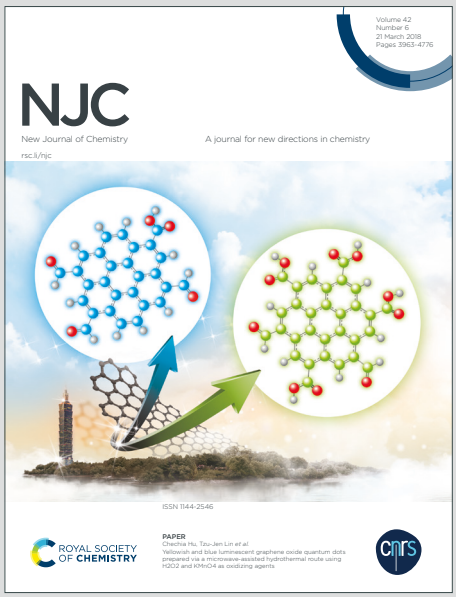

This is an Accepted Manuscript, which has been through the Royal Society of Chemistry peer review process and has been accepted for publication.

Accepted Manuscripts are published online shortly after acceptance, before technical editing, formatting and proof reading. Using this free service, authors can make their results available to the community, in citable form, before we publish the edited article. We will replace this Accepted Manuscript with the edited and formatted Advance Article as soon as it is available.

You can find more information about Accepted Manuscripts in the Information for Authors.

Please note that technical editing may introduce minor changes to the text and/or graphics, which may alter content. The journal's standard Terms & Conditions and the Ethical guidelines still apply. In no event shall the Royal Society of Chemistry be held responsible for any errors or omissions in this Accepted Manuscript or any consequences arising from the use of any information it contains.

Supramolecular assembly and spectroscopic characterization of indolenine - barbituric acid zwitterions

Abdul Qaiyum Ramle [a]*, Edward R. T. Tiekink [b]*, Chee Chin Fei [c], Nurhidayatullaili Muhd Julkapli [c], Wan Jefrey Basirun [a]*

[a] Department of Chemistry, University of Malaya, 50603, Kuala Lumpur, Malaysia.

[b] Research Centre for Crystalline Materials, School of Science and Technology, Sunway University, 47500, Bandar Sunway, Selangor Darul Ehsan, Malaysia.

[c] Nanotechnology and Catalysis Research Centre, University of Malaya, 50603, Kuala Lumpur, Malaysia.

*Corresponding authors:

jeff@um.edu.my (W. J. Basirun), qaiyum@um.edu.my (A. Q. Ramle), edwardt@sunway.edu.my (E. R. T. Tiekink)

Abstract

A series of indolenine and barbituric acid zwitterion scaffolds were synthesized with a maximum yield of 98% *via* the formation of C–C single bond. The structures were unambiguously elucidated by various spectroscopic techniques such as ^{1}H, ^{13}C NMR (1D, 2D), FT-IR and high-resolution mass spectrometry (HRMS). Single crystal X-ray crystallography analysis on **22**, as the **22.DMF** 1:1 solvate, confirms the presence of well-separated iminium and enolate centres, and also confirms that the BA ring is highly twisted with respect to the indolenine ring due to steric hindrance. The presence of N–H···O and N–H···O^{-} groups favour a 1D-supramolecular assembly in the solid-state. The orange or yellow solutions of the zwitterion exhibit an intense molar absorption coefficient, ε ranging between 0.21×10^{4} and 2.93×10^{4} M^{-1} cm^{-1} in the UV-vis region. Furthermore, the Intramolecular Charge Transfer (ICT) peak of zwitterion displays a hypsochromic shift in absorption behavior when the polarity of the solvent increases. Moreover, treatment of small amount of trifluoroacetic acid (TFA) to the DMF solution of **19** resulted in the protonation of an enolate of BA ring. This fundamental work provides valuable structural design and information for the construction of supramolecular chemistry and synthetic dyes based on indolenine substituted BA derivatives.

Keywords: Indolenine-barbituric acid, Zwitterion, Supramolecular chemistry, UV-visible spectroscopy.

Introduction

Since 1864, barbituric acid (BA) has been used in organic and medical chemistry due to its impressive biological activities.[1-4] BA is an effective fluorescence probe for chemosensors and for live-cell bio-imaging detections.[5-8] The reactivity of BA in organic reactions is characterized by its tendency to form both coordination and hydrogen bonds, which enables it as building blocks for supramolecular assemblies with distinctive shape, size and topology.[9-13] BA readily undergoes keto-enol tautomerism and forms zwitterions with pyridinium,[14-16] isoquinolinium,[17] imidazolium,[18, 19] codeinone[20] and tetramethylguanidium.[21] Interestingly, the formation of BA zwitterions could be achieved by visible-light irradiation.[22] Although reactions of BA have been extensively investigated, there are very few reports on the formation mechanism of BA zwitterion.

Studies have shown that BA derivatives have excellent photostability and exhibit good intramolecular charge transfer (ICT) properties.[23-25] The charge transfer property of BA produces interesting UV-vis and near infrared (NIR) spectroscopic characteristics. Thus, the combination of BA with different types of aromatic heterocyclic scaffolds *via* the Knoevenagel condensation reaction is a powerful synthetic approach in the design of push-pull chromophores. For example, indoleninyl-barbiturates exhibit intense and sharp absorptions in the NIR region with high molar extinction coefficients and ICT properties.[26, 27] Interestingly, the spectral properties of the indolenine chromophores can be tailored by controlling the types of donor and acceptor units, π-conjugated linkers or the heteroaromatic π-systems in the molecular frameworks.[28, 29] The structural modification alters the HOMO and LUMO energy gaps, thus enables the tuning of optical properties for specific applications. Hence, the unique structural features of indolenines make them suitable as active substances for various applications in modern electronic devices.[30-32]

In the design of *N*-heterocyclic dyes, herein we report a new series of indolenine-BA zwitterions. The structures were characterized by spectroscopic techniques and confirmed by single crystal X-ray crystallographic analysis. The relationship between different electron donating group (EDG) and electron withdrawing group (EWG) substituents towards the photophysical properties were investigated.

View Article Online
DOI: 10.1039/D0NJ04357E

Results and discussions

a. Synthesis and characterizations

The starting materials of compounds **1** – **5** were prepared as described elsewhere.[33, 34] The *N*-methylation and *N*-benzylation of **1** – **5** were performed under mild basic conditions to afford the diformyl **6** – **9** and **11** – **15**. Then, compound **9** was converted to **10** *via* the base hydrolysis. The synthetic scheme for the intermediate compounds is outlined in Scheme S1 (ESI). Finally, the Knoevenagel condensation of diformyl **6** – **15** with BA *via* refluxing in methanol afforded the zwitterions **16** – **25**. As shown in Scheme 1, the *N*-methyl zwitterions **17**, **19** and **20** featuring with EWG groups (Cl, COOEt, COOH) on the indolenine ring were isolated in lower yields compared to reference **16**. In contrast, the zwitterions **18** and **21** bearing with EDG (OMe, C_4H_4) gave higher product yields compared to reference **16**. These results conclude that the electronic nature of the EDG enhances the reactivity on the indolenine ring to form the zwitterions. Next, the synthetic scope was extended to *N*-benzyl zwitterions, **22** – **25**. However, the relationship between substituent effects toward yields obtained among these zwitterions could not be established due to successful preparation of several compounds under this synthetic protocol. Nevertheless, the presence of benzyl group on the indolenine ring gave the products in between 52 – 98% isolated yields.

All compounds are stable in both the solid and solution states at ambient temperature with melting points more than 216 ^{o}C. The zwitterions **22** – **25** are soluble in THF, dioxane, DMF, DMSO but is partially soluble in alcohols. Meanwhile, zwitterions **16** – **21** are only soluble in DMF and DMSO.

View Article Online
DOI: 10.1039/D0NJ04357E

Scheme 1: Substrate scope of indolenine-BA zwitterions [a,b]

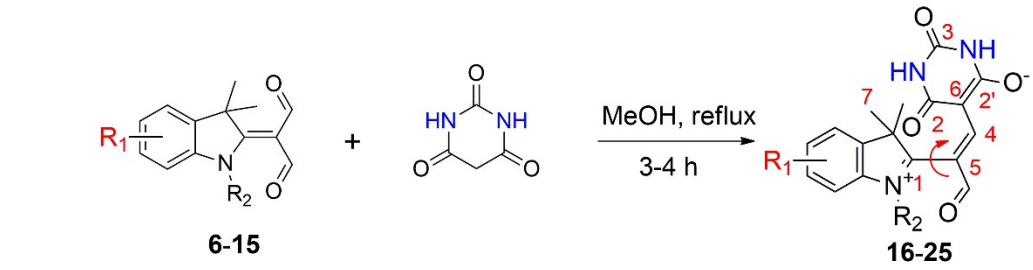

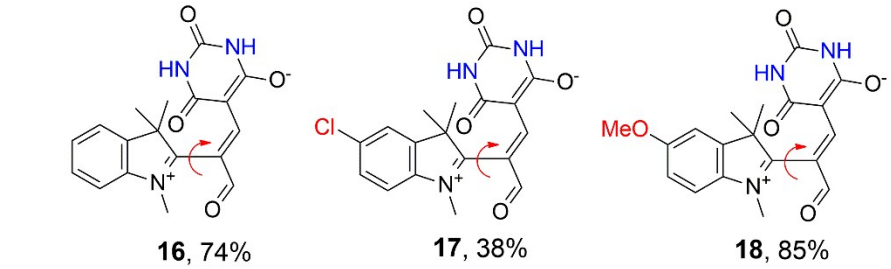

16, 74% **17**, 38% **18**, 85%

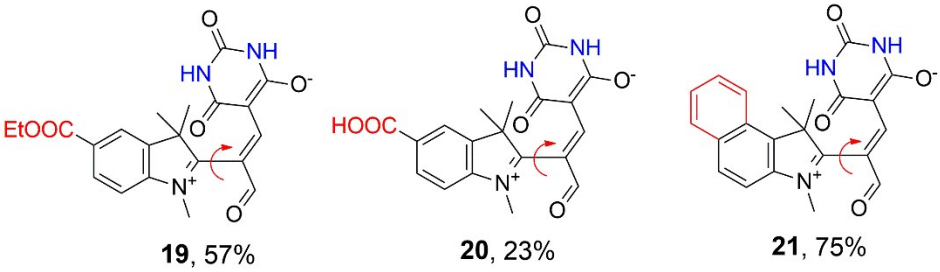

19, 57% **20**, 23% **21**, 75%

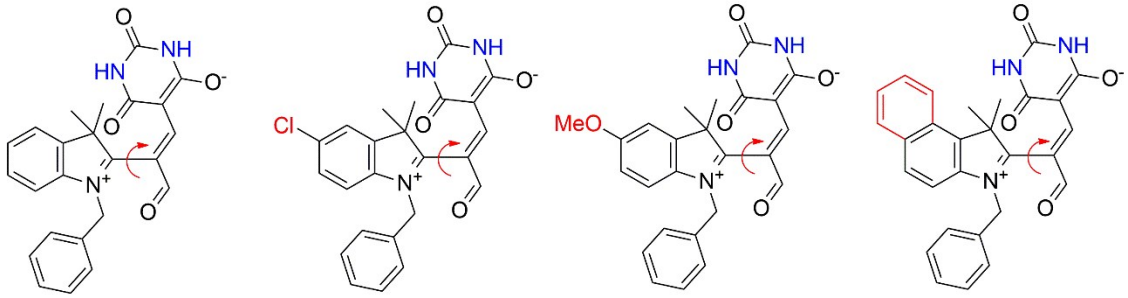

22, 64% **23**, 98% **24**, 52% **25**, 76%

[a] Reaction conditions: **6** – **15** (1 equiv.), BA (1.1 equiv.) in MeOH, reflux, 3-4 h. [b] Isolated yields.

The structures of zwitterions **16** – **25** were determined by NMR spectroscopy and their molecular masses were confirmed by HRMS analyses. The ^{1}H NMR spectra of all zwitterions show two distinctive N─H protons as singlets between δ 10.11 – 10.48 ppm, indicating a strong electronegative effect. The singlet proton signals between δ 9.21 – 9.33 ppm and between δ 7.99 – 8.12 ppm correspond to the aldehyde and olefinic groups, respectively. The chemical shifts for the presence of *N*-methyl protons and *N*-benzyl protons occur between δ 3.60 – 3.77 ppm and δ 5.28 – 5.47 ppm, respectively. Apart from that, the singlet between δ 1.31 – 1.68 ppm is assigned to the methyl protons.

The HMBC NMR data (Fig. S43, ESI) indicates that the de-shielded iminium carbon (C-1) peak occurs between δ 190.44 – 196.16 ppm. The three carbonyl signals of the BA moiety (C-2, C-2', C-3) resonate between δ 151.24 – 164.90 ppm. The spectral data reveal that the olefinic peak (C-4) appears around δ 152.28 – 153.05 ppm, whereas the carbon signal (C-5) occurs between δ 108.48 – 109.57 ppm. Interestingly, the chemical shift of methylene BA, (C-6) occurs between δ 94.38 – 96.02 ppm which is shielded compared to the reported structure due to an enhanced nucleophilic character.[35] Surprisingly, the chemical shifts of dimethyl carbons (C-7) appear at relatively lower resolutions in the ^{13}C NMR spectrum. However, their correlations with the methyl protons are clearly indicated in the HSQC experiment (Fig. S44, ESI).

The FT-IR spectra of **16** – **25** show a strong band intensity at around 1687 – 1716 cm^{-1}, typically attributed to the C=O aldehyde band. The formation of the iminium units is confirmed by the sharp stretching peak at around 1512 – 1657 cm^{-1}. The peaks at 1709 cm^{-1} and 1717 cm^{-1} correspond to the C=O ester **19** and carboxylic acid **20**, respectively. Interestingly, the N─H stretching frequencies are not observed at regions close to 3300 cm^{-1}, due to the N─H···O intermolecular hydrogen bonding[36, 37] in the BA. The C=O stretching modes of BA are observed at around 1615 – 1669 cm^{-1}, as expected from previous reports.[38, 39]

View Article Online
DOI: 10.1039/D0NJ04357E

b. X-ray crystallography

The molecular structure of **22** was established by X-ray crystallography from the crystals of the 1:1 solvate with DMF, i.e. **22.DMF**. The molecular structure of **22** is shown in Fig. 1 and the selected geometric parameters are tabulated in Table 1. A key point in the structure is that the C24–O4 bond length is significantly longer compared to the C22–O2 and C23–O3 bonds, thus providing geometric evidence for the formation of an enolate ion with the negative charge localized at the O4 atom. Conversely, the C1–N1 bond length is significantly shorter than any of the other C–N bonds, consistent with the formation of an iminium centre. Further, the sum of the angles subtended at the N1 amounts to 360.0°. In addition, each of the aldehyde–O1 [3.0763(19) Å] and amide–O2 [2.9907(17) Å] atoms are orientated to form close contact with the iminium–N1 atom, indicative of electrostatic attraction. Thus, from the structural study it can be concluded that the positive charge localized on the iminium-nitrogen cation is neutralized by the negative charge in the resonance stabilized BA moiety (Scheme 2).

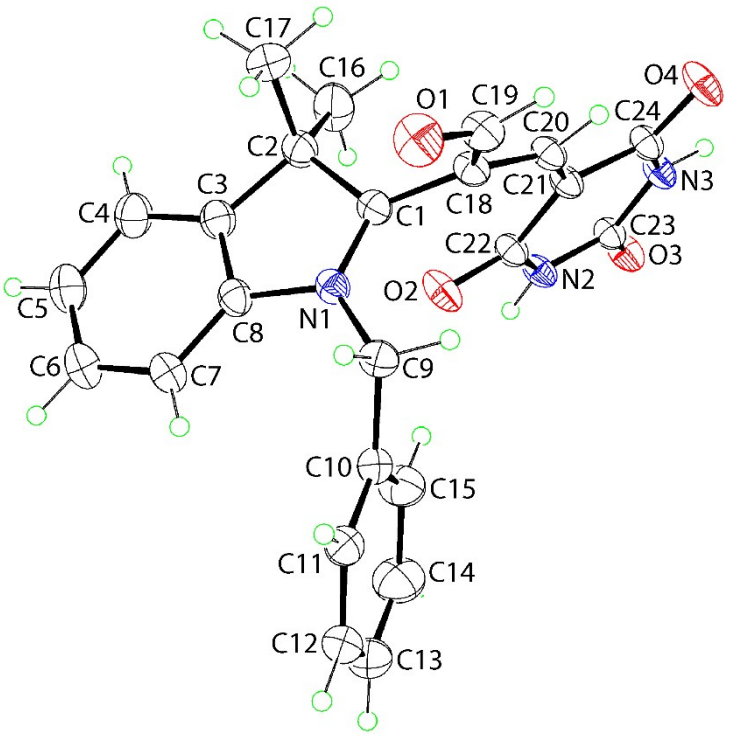

Fig. 1: Molecular structure of **22** in **22.DMF**, showing atomic labelling and displacement parameters at the 35% probability level. The DMF molecule is omitted.

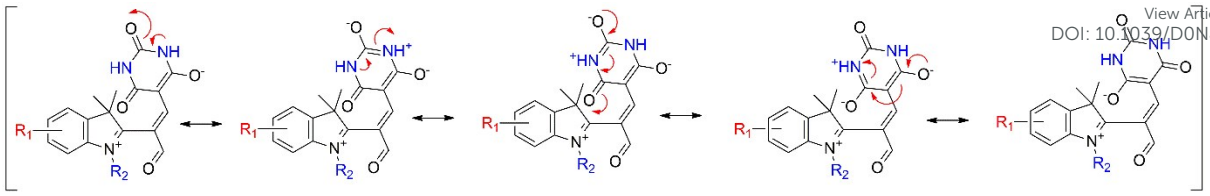

Scheme 2: General resonance scheme for zwitterions.

With regards to the conformation, the structural analysis shows that the indolenine fragment is rotated out of the attached propene plane to avoid steric hindrance, as seen in the value of the N1–C1–C18–C20 torsion angle of 123.84(17)°. As a result, the sequence of C1–C18, C18–C20 and C20–C21 bonds exhibits substantial bond length alteration due to the loss of π-conjugation.[40, 41]

Table 1: Selected bond lengths (Å), bond angles (°) and torsion angles (°) for **22**

Bond lengths			
N2 – C22	1.3898(17)	C1 – N1	1.3105(18)
N2 – C23	1.3632(18)	C1 – C18	1.465(2)
N3 – C23	1.3643(18)	C18 – C19	1.4531(19)
N3 – C24	1.3886(17)	C18 – C20	1.3703(19)
C19 – O1	1.2190(19)	C20 – C21	1.4092(18)
C22 – O2	1.2280(17)	C21 – C22	1.4356(19)
C23 – O3	1.2237(16)	C21 – C24	1.4359(19)
C24 – O4	1.2424(17)		
Bond angles			
C1 – N1 – C8	110.82(12)	C20 – C21 – C22	122.69(12)
C23 – N2 – C22	125.86(11)	C24 – C21 –C22	119.40(12)
C23 – N3 – C24	125.31(12)	N1 – C1 – C18	124.32(13)
C18 – C20 – C21	133.72(13)	N2 – C22 – C21	116.52(12)
C20 – C18 – C1	127.07(12)	N3 – C23 –N2	115.76(11)
C20 – C21 – C24	117.78(12)	N3 – C24 – C21	117.00(12)
Torsion angles			
N1 – C1 – C18 – C20	123.84(17)	C1 – C18 – C20 – C21	−13.9(3)
N1 – C1 – C18 – C19	−64.22(19)	C18 – C20 – C21 – C24	173.02(16)
C2 – C1 – C18 – C19	98.03(17)	C18 – C20 – C21 – C22	−11.3(3)
C2 – C1 – C18 – C20	−73.9(2)		

Table 2: Hydrogen-bond geometry in the crystal of **22.DMF**

D–H···A	H···A (Å)	D···A (Å)	D – H···A (°)	Symmetry operation
N2–H2n···O3^{i}	2.051(14)	2.8965(17)	171.7(16)	2-*x*, 1-*y*, 2-*z*
N3–H3n···O4^{ii}	1.984(15)	2.8514(17)	172.6(16)	2-*x*, -*y*, 2-*z*

The most notable feature of the molecular packing in the crystal of **22.DMF** is the formation of cooperative pairs of amide-N–H···O hydrogen bonds between centrosymmetrically related BA residues (Table 2). It is noted that the hydrogen bond of the formally enolate-O4 atom is significantly shorter compared to the amide-O3 atom consistent with the former being, at least partially, a charge-assisted amide-N–H···O^{-} hydrogen bond. The hydrogen bonding leads to the formation of eight-membered {…OCNH]$_2$ synthons which are concatenated and generate a flat, supramolecular tape with a *zig-zag* topology (Fig. 2). The tapes are assembled into supramolecular layers parallel to (-1 0 1) *via* the methylene-C–H···O(aldehyde) interactions and are connected to this array, *via* the methyl-C–H···O(DMF) contacts, (ESI, Fig. S54c). The V=BA-O2 atom has no charge role in the supramolecular association. Nevertheless, this atom is involved in a short intramolecular phenyl-C–H···O2 contact [H15···O2 = 2.35 Å with angle at H15 = 164°].

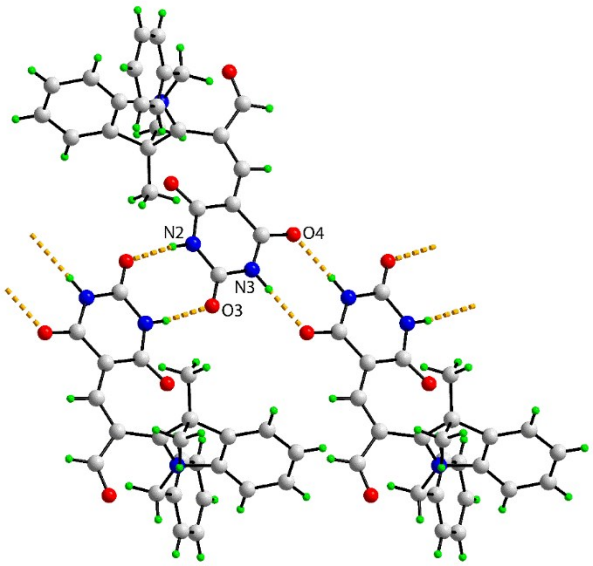

Fig. 2: A perspective view of the one-dimensional supramolecular tape in the crystal of **22.DMF** sustained by amide-N–H···O(amide) hydrogen bonding.

View Article Online
DOI: 10.1039/D0NJ04357E

c. UV-vis absorption spectroscopy

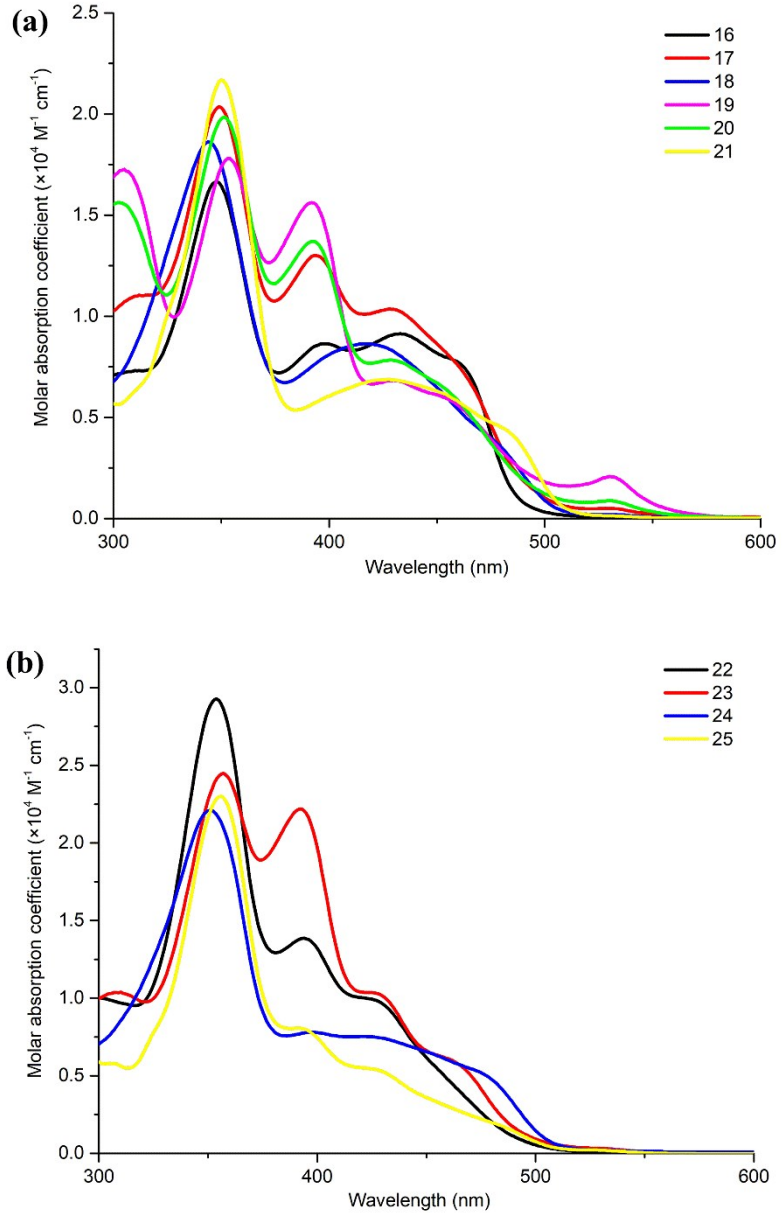

Fig. 3: (a) UV-vis spectra for zwitterions **16** - **21** and (b) **22** - **25** in dilute DMF (50 µM).

Table 3: Photophysical parameters of zwitterion **16** – **25**.

Zwitterion	Absorption, λ_{max} (nm) / ε ($\times 10^4$ M^{-1} cm^{-1})	λ_{onset} (nm)	FWHM (nm)	E_{gap} (eV) = 1240 / λ_{onset}
16	348 (1.66)	488	25.5	2.54
17	349 (2.04), 394 (1.30)	497	23.4, 16.5	2.50
18	344 (1.86)	510	37.5	2.43
19	303 (1.72), 352 (1.78), 392 (1.55), 530 (0.21)	558	29.7, 25.3, 27.3, 19.5	2.22
20	303 (1.56), 352 (1.98), 392 (1.37)	505	28.5, 22.2, 18.6	2.46
21	351 (2.17)	510	29.3	2.43
22	354 (2.93)	490	26.6	2.53
23	357 (2.45), 393 (2.22)	499	30.5, 25.4	2.49
24	351 (2.21)	506	38.6	2.45
25	356 (2.30)	507	31.7	2.45

The UV-vis absorption spectra of zwitterions **16** – **25** were measured in DMF at room temperature and their photophysical data are summarized in Table 3. The E_{gap} values of the zwitterions were calculated from the extrapolation of the absorption spectrum.[42] Generally, the absorption region between 300 nm to 380 nm is assigned to the π-π* electronic excitation of the indolenine chromophore unit, whereas a broad absorption profile in the Soret band region is attributed to the ICT transition from the indolenine donor to the BA acceptor moiety.[43-45] However, the twisted conformation of the zwitterions weakened the ICT properties on the absorption spectra due to inadequate π-conjugation. As shown in Fig. 3(a), the comparison of the spectra of zwitterions **17** and **18** with that of **16** reveals a bathochromic shift in the absorption of onset wavelength upon insertion of -Cl or -OMe substituents on the indolenine ring. Interestingly, introduction of -COOEt and -COOH groups of **19** and **20**, respectively, have significant effect on the electronic properties of the molecules, where the three intense absorption peaks appear at similar wavelengths at 303, 352 and 392 nm. The difference is the presence of an additional weak Q-band peak at 530 nm for **19** which corresponds to the n-π* transition of the conjugated carbonyl ester group. Furthermore, the spectrum of **21** displays a slight bathochromic shift for both the absorption maximum and the onset wavelengths, which suggests the extension of the π-conjugation system as compared to **16**. This results in an energy band gap decrease of 0.11 eV of **21**.

View Article Online
DOI: 10.1039/D0NJ04357E

As depicted in Fig. 3(b), zwitterions **22** – **25** demonstrate a hyperchromic shift due to the presence of benzyl group in their structures. This is possibly due to the alteration of the molecular structure which enhances the interaction with light. However, none of these zwitterions exhibit significant fluorescence properties. This is due to the twisted geometrical structure which leads to an orbitally decoupled π-systems of the donor indolenine and BA acceptor units.[46]

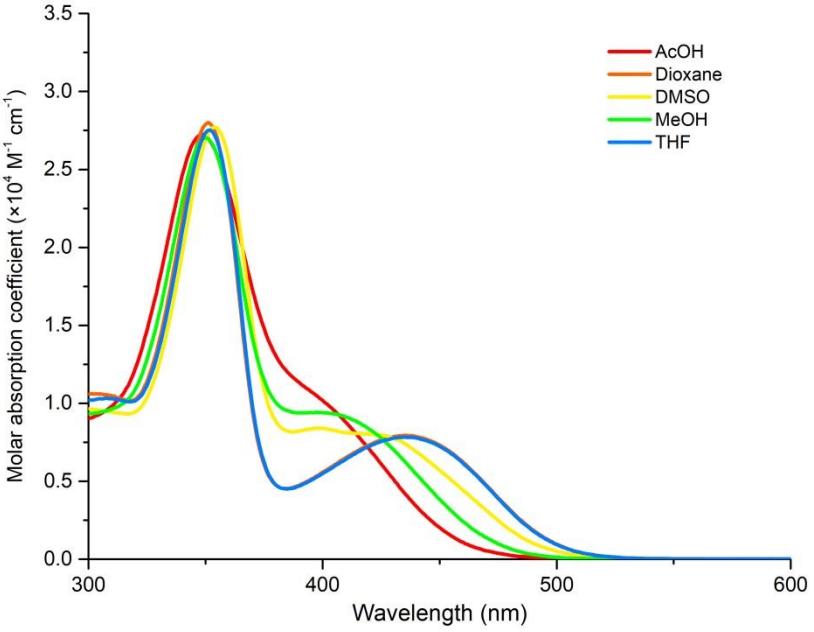

Fig. 4: UV-vis absorption spectra of **22** (50 μM) recorded in different solvents.

The photophysical parameters of **22** were further examined in different solvents and summarized in Table S2 (ESI). As illustrated in Fig. 4, no obvious π-π* peak shifting was observed in the region of 350 nm. The electronic properties of **22** in THF and dioxane solvents are almost similar despite the different polarities possessed by the two solvents. Clearly, the broad ICT absorption peak centred at 435 nm in THF or dioxane progressively shifts to shorter wavelength (hypsochromic shift) with increasing the solvent polarity from DMSO to methanol and acetic acid. This characteristic suggests that the ground state of the molecules is better stabilized by polar solvents.[47] The solvation effect is significantly observed in methanol and acetic acid, which may be due to the intermolecular hydrogen bonding interaction through the N-H groups of BA moiety.[23] Furthermore, no protonation of the enolate has occurred in the acetic acid solvent as indicated in the spectrum due to the high stability and resistivity of the negatively charged BA ring to acetic media.[48] Overall, the calculated molar absorption coefficients and E_{gap} values of **22** in various solvents are between 0.78 – 2.93 × 10^4 M^{-1} cm^{-1} and 2.48 – 2.71 eV, respectively. Thus, these values suggest suitable utilization of the zwitterions for various optoelectronic devices.[49]

d. Protonation of 19 by TFA

TFA is a common acid used for the protonation reaction due to its strong acidity properties and good solubility in organic solvents.[50, 51] In the DMF solution, the zwitterion **19** displays a color change from orange to yellow with the addition of an equivalent of TFA. The UV-vis absorption spectrum exhibits a slight hypsochromic shift upon addition of an equivalent of TFA (Fig. S56, ESI). The two new intense absorption peaks appear at 351 nm and 450 nm are attributed to the π-π* transition in the indolenine ring and the ICT transition from the donor to the acceptor moiety, respectively. In addition, multiple isosbestic points are detected in the spectrum, which confirms that the protonation of the enolate of BA ring has taken place in the presence of TFA. However, no further changes are observed on the color of the solution and the spectral pattern after the addition of TFA in excess (10 equiv.). This indicates that the protonation reaction is completed. The calculated E_{gap} value for the protonated **19** is 2.45 eV, which is higher than that of the neutral **19** (Table 3).

Furthermore, the addition of TFA to the solution of **19** in deuterated DMSO was also studied by ^{1}H NMR spectroscopy. As depicted in Fig. S57 (ESI), the spectrum shows two distinctive N-H protons at δ 10.53 ppm and 10.35 ppm, which is slightly shifted to the lower field as compared to the neutral **19** probably due to the reduction of the electron density in the BA ring.

Conclusions

In summary, we have prepared a series of new indolenine substituted BA zwitterions in good yields through a simple and facile synthetic protocol. All compounds are successfully characterized by spectroscopic analyses. Single X-ray crystallography analysis confirms that the zwitterion possesses the twisted conformation and stabilizes into a 1D-supramolecular assembly *via* intermolecular hydrogen bonding. The photophysical studies reveal that all zwitterions demonstrated broad absorption profile between 300 nm and 530 nm, and their electronic transitions are highly dependent on the electronic substituents on the indolenine ring. Interestingly, the ICT band of zwitterion exhibits a hypsochromic shift behavior as the solvent polarity increases. The protonation effect of zwitterion by addition of an equivalent of TFA dramatically tunes the electronic chromophores and the spectral properties. Further work on the synthetic approaches such as extension of the π-conjugation based indoleninyl-

barbiturate frameworks and their application in electronic devices are currently under investigation.

Experimental Section

Materials

All chemicals were purchased in high quality grade from Sigma Aldrich and Merck Millipore Companies, Malaysia. The solvents were used without further purifications unless otherwise noted.

Instrumentations

The NMR spectra were recorded using a JEOL ECX 400II MHz or a Bruker AVANCE III 600 MHz spectrometers measured in deuterated $CDCl_3$ or DMSO as the solvents. Chemical shifts (δ) and coupling constant (J) values are reported in ppm and Hz units, respectively. The FT-IR spectra were performed on a Perkin-Elmer Spectrum 400 IR spectrometer. Melting points were measured on a Mel-Temp II instrument in open capillaries tube. The Agilent 6530 Accurate-Mass Q-TOF LC/MS system was used to determine the molecular ion fragments of the compounds. The UV-vis absorption spectra were measured at room temperature on a Shimadzu UV-2600 UV-VIS spectrophotometer. The OriginPro 2016 64-bit software was used to calculate the FWHM of the UV-vis absorption spectra.

X-ray crystallography

X-ray intensity data for a yellow crystal of **22.DMF** (0.10 × 0.20 × 0.20 mm) were measured at T = 293 K on an Agilent Technologies Supernova Dual diffractometer with Atlas detector fitted with CuKα radiation (λ = 1.54184 Å). Data reduction, including absorption correction, was accomplished with CrysAlisPro.[52] The structure was solved by direct-methods[53] and refined (anisotropic displacement parameters and C-bound H atoms in the riding model approximation) on F^2.[54] The N-bound H atoms were refined with the N–H bond lengths constrained to 0.86 ± 0.01 Å, and with U_{iso}(H) = 1.2U_{eq}(N). A weighting scheme of the form $w = 1/[\sigma^2(F_o^2) + (0.096P)^2 + 0.193P]$ where $P = (F_o^2 + 2F_c^2)/3$) was introduced at the end of the refinement. The molecular structure diagram was generated with ORTEP for Windows[55] with 35% displacement ellipsoids, and the packing diagrams were drawn with DIAMOND.[56]

Crystal data for **22.DMF**: $C_{24}H_{21}N_3O_4$, C_3H_7NO, M = 488.53, triclinic, $P\bar{1}$, a = 8.2773(3), b = 10.4031(3), c = 15.3328(5) Å, α = 80.801(3)°, β = 79.757(3)°, γ = 73.423(3)°, V = 1236.89(7) Å^3, Z = 2, D_x = 1.312 g cm^{-3}, $F(000)$ = 516 and μ = 0.753 mm^{-1}. No. reflections measured = 20020 (θ_{max} = 74.3º), no. independent reflections = 4935, no. reflections with $I \geq 2\sigma(I)$ = 4159, R (obs. data) = 0.051 and wR_2 (all data) = 0.151.

Crystallographic data for compound **22.DMF** reported in this paper have been deposited with the Cambridge Crystallographic Data Centre (CCDC) as supplementary publication nos. CCDC-2023454. These data can be obtained free of charge *via* www.ccdc.cam.ac.uk/getstructures.

General procedure for the preparation of 6 – 11.

A solution of diformyl **1** – **5** (1 equiv.), anhydrous K_2CO_3 (3 equiv.), and CH_3I (1.5 equiv.) in a minimum amount of DMF solution was stirred at room temperature for 20-24 h. The progress of the reaction was monitored by thin-layer chromatography (TLC). Upon completion, water was added and extracted with ethyl acetate. The organic layer was dried over $MgSO_4$ and the solvent removed under reduced pressure. The residue was purified by column chromatography using hexane/ethyl acetate (v/v = 1 – 2:1) as the eluent to afford the pure product.

Compound 6: Purple solid. Yield: 56%. m.p = 120 – 121 ºC. ^{1}H NMR (400 MHz, $CDCl_3$): δ 9.63 (s, 2H, CHO), 7.39 (m, 3H, J = 7.6, 2.0 Hz, Ar-H), 7.22 (dd, 1H, J = 8.0 Hz, 2.8 Hz, Ar-H), 3.54 (s, 3H, CH_3), 1.66 (s, 6H, CH_3). ^{13}C NMR (100 MHz, $CDCl_3$): δ 187.97 (CHO), 183.76 (C-N), 142.67, 142.33, 128.35, 126.90, 122.07, 112.19, 109.94, 52.72, 38.44, 25.14. FT-IR (ATR): 3027, 2976, 2934, 2837, 1624, 1510, 1482, 1470, 1391, 1375, 1224, 766, 733 cm^{-1}. HRMS (ESI): m/z [M+H]$^+$ calcd $C_{14}H_{16}NO_2$: 230.1186; found: 230.1182.

Compound 7: Brown solid. Yield: 57%. m.p = 134 – 135 ºC. ^{1}H NMR (400 MHz, $CDCl_3$): δ 9.67 (s, 2H, CHO), 7.37 (dd, 1H, J = 8.8, 2.4 Hz, Ar-H), 7.32 (d, 1H, J = 2.0 Hz, Ar-H), 7.14 (d, 1H, J = 8.0 Hz, Ar-H), 3.52 (s, 3H, CH_3), 1.69 (s, 6H, CH_3). ^{13}C NMR (100 MHz, $CDCl_3$): δ 187.82 (CHO), 183.18 (C-N), 143.95, 141.34, 132.74, 128.51, 122.76, 113.06, 110.14, 52.71, 38.73, 24.98. FT-IR (ATR): 2940, 2744, 2720, 1615, 1495, 1472, 1445, 1403, 1381, 1173, 815, 761 cm^{-1}. HRMS (ESI): m/z [M+H]$^+$ calcd $C_{14}H_{15}ClNO_2$: 264.0786; found: 264.0791.

Compound 8: Brown solid. Yield: 48%. m.p = 144 – 146 °C. ^{1}H NMR (400 MHz, $CDCl_3$): δ 9.53 (s, 2H, CHO), 7.17 (d, 1H, J = 9.2 Hz, Ar-H), 6.89 (m, 2H, J = 4.0, 2.8 Hz, Ar-H, overlapped), 3.84 (s, 3H, OMe), 3.56 (s, 3H, CH_3), 1.66 (s, 6H, CH_3). ^{13}C NMR (100 MHz, $CDCl_3$): δ 187.59 (CHO), 183.18 (C-N), 159.52, 144.44, 136.00, 113.21 (2C), 109.59, 108.57, 55.98, 53.20, 38.28, 25.10. FT-IR (ATR): 2978, 2841, 2761, 1609, 1515, 1487, 1393, 1306, 1131, 1024, 807, 737 cm^{-1}. HRMS (ESI): m/z $[M+H]^+$ calcd $C_{15}H_{18}NO_3$: 260.1281; found: 260.1285.

Compound 9: Purple solid. Yield: 88%. m.p = 88 – 90 °C. ^{1}H NMR (400 MHz, $CDCl_3$): δ 9.77 (s, 2H, CHO), 8.11 (dd, 1H, J = 8.4, 1.6 Hz, Ar-H), 7.98 (s, 1H, Ar-H), 7.22 (d, 1H, J = 8.4 Hz, Ar-H), 4.41 (q, 2H, CH_2), 3.53 (s, 3H, CH_3), 1.72 (s, 6H, CH_3), 1.43 (t, 3H, CH_3). ^{13}C NMR (100 MHz, $CDCl_3$): δ 188.09 (CHO), 183.76 (C-N), 165.83 (C=O), 146.41, 142.04, 130.65, 128.63, 123.26, 111.53, 110.80, 61.54, 52.16, 38.90, 25.26, 14.44. FT-IR (ATR): 2976, 2933, 2741, 2705, 1707, 1641, 1287, 1235, 1100, 1024, 770, 760, 745 cm^{-1}. HRMS (ESI): m/z $[M+H]^+$ calcd $C_{17}H_{20}NO_4$: 302.1387; found: 302.1389.

Compound 10: A solution of **9** (1 equiv.) and NaOH (5 equiv.) in MeOH/water (v/v = 2:1) was stirred at room temperature for 12 h and the progress of the reaction was monitored by TLC. Upon completion, MeOH was removed under reduced pressure and added with water. The mixture was acidified to pH = 4-5 with 5% HCl (aq). The resulting precipitate was filtered, washed with hot distilled water and dried at 60 °C. Brown solid. Yield: 46%. m.p = 201 – 203 °C. ^{1}H NMR (400 MHz, DMSO): δ 9.70 (s, 2H, CHO), 8.05 (s, 1H, Ar-H), 8.00 (d, 1H, J = 8.0 Hz, Ar-H), 7.51 (d, 1H, J = 8.0 Hz, Ar-H), 3.44 (s, 3H, CH_3), 1.62 (s, 6H, CH_3). ^{13}C NMR (100 MHz, DMSO): δ 187.93 (CHO), 183.10 (C-N), 167.82 (C=O), 146.78, 142.13, 130.77, 128.81, 123.48, 112.79, 110.89, 51.85, 39.29, 25.05. FT-IR (ATR): 2934, 2630, 1703, 1658, 1594, 1386, 1221, 1199, 767, 739 cm^{-1}. HRMS (ESI): m/z $[M+H]^+$ calcd $C_{15}H_{16}NO_4$: 274.1074; found: 274.1076.

Compound 11: Brown solid. Yield: 76%. m.p = 173 – 175 °C. ^{1}H NMR (400 MHz, $CDCl_3$): δ 9.65 (s, 2H, CHO), 8.12 (d, 1H, J = 8.8 Hz, Ar-H), 7.98 (m, 2H, J = 8.0, 4.4 Hz, Ar-H), 7.66 (td, 1H, J = 6.8, 1.6 Hz, Ar-H), 7.55 (td, 1H, J = 6.8, 0.8 Hz, Ar-H), 7.48 (d, 1H, J = 8.4 Hz, Ar-H), 3.69 (s, 3H, CH_3), 1.97 (s, 6H, CH_3). ^{13}C NMR (100 MHz, $CDCl_3$): δ 188.00 (CHO), 185.53 (C-N), 139.55, 136.21, 132.80, 130.30, 130.04, 127.90, 127.76, 125.94, 123.01, 111.32, 109.58, 54.60, 38.78, 24.26. FT-IR (ATR): 2977, 2923, 2843, 1613, 1510,

1394, 1244, 1186, 804, 751, 750 cm^{-1}. HRMS (ESI): *m/z* $[M+H]^+$ calcd $C_{18}H_{18}NO_2$: 280.1332; found: 280.1350.

General procedure for the preparation of 12 – 15.

A solution of diformyl **1** – **3**, **5** (1 equiv.), K_2CO_3 (3 equiv.), KI (1.5 equiv.), benzyl bromide (1.5 equiv.) in a minimum amount of DMF was stirred at room temperature for 110-120 h. The progress of the reaction was monitored by TLC. Upon completion, water was added and extracted with ethyl acetate. The organic layer was dried over $MgSO_4$ and the solvent removed under reduced pressure. The residue was purified by column chromatography using hexane/ ethyl acetate (v/v = 1-2:1) as the eluent to afford the pure product.

Compound 12: Brown solid. Yield: 36%. m.p = 112 – 113 °C. ^{1}H NMR (400 MHz, $CDCl_3$): δ 9.63 (s, 2H, CHO), 7.33 (m, 1H, *J* = 6.0, 2.0 Hz, Ar-H), 7.29 (m, 3H, *J* = 8.0, 2.4 Hz, Ar-H), 7.22 (m, 2H, *J* = 4.8, 3.2 Hz, Ar-H), 7.14 (d, 2H, *J* = 7.2 Hz, Ar-H), 7.01 (dd, 1H, *J* = 5.6, 2.4 Hz, Ar-H), 5.25 (s, 2H, CH_2), 1.74 (s. 6H, CH_3). ^{13}C NMR (100 MHz, $CDCl_3$): δ 188.05 (CHO), 184.51 (C-N), 142.84, 141.53, 133.96, 129.17, 128.50, 127.97, 127.28, 126.50, 122.04, 114.05, 110.75, 54.50, 52.79, 25.13. FT-IR (ATR): 3029, 2964, 2922, 2769, 1607, 1458, 1445, 1424, 1402, 1174, 748, 737, 694 cm^{-1}. HRMS (ESI): *m/z* $[M+H]^+$ calcd $C_{20}H_{20}NO_2$: 306.1489; found: 306.1491.

Compound 13: Orange solid. Yield: 21%. m.p = 132 – 133 °C. ^{1}H NMR (400 MHz, $CDCl_3$): δ 9.57 (s, 2H, CHO), 7.32-7.28 (m, 4H, *J* = 10.0, 2.4 Hz, Ar-H), 7.19 (dd, 1H, *J* = 8.4, 2.0 Hz, Ar-H), 7.14 (d, 1H, *J* = 2.4 Hz, Ar-H), 7.12 (d, 1H, *J* = 1.2 Hz, Ar-H), 6.94 (d, 1H, *J* = 8.4 Hz, Ar-H), 5.22 (s, 2H, CH_2), 1.74 (s, 6H, CH_3). ^{13}C NMR (100 MHz, $CDCl_3$): δ 187.17 (CHO), 184.43 (C-N), 144.55, 139.91, 133.14, 133.00, 129.41, 128.89, 128.36, 127.29, 122.86, 115.42, 110.51, 54.93, 53.31, 24.80. FT-IR (ATR): 2974, 2931, 2750, 2719, 1615, 1449, 1421, 1373, 1182, 1082, 965, 802, 746, 706 cm^{-1}. HRMS (ESI): *m/z* $[M+H]^+$ calcd $C_{20}H_{19}ClNO_2$: 340.1099; found: 340.1101.

Compound 14: Yellow solid. Yield: 16%. m.p = 128 – 130 °C. ^{1}H NMR (400 MHz, $CDCl_3$): δ 9.43 (s, 2H, CHO), 7.31 (m, 3H, *J* = 8.0, 2.0 Hz, Ar-H), 7.18 (dd, 2H, *J* = 6.0, 1.6 Hz, Ar-H), 6.98 (d, 1H, *J* = 8.8 Hz, Ar-H), 6.88 (d, 1H, *J* = 2.8 Hz, Ar-H), 6.73 (dd, 1H, *J* = 8.4, 2.0 Hz, Ar-H), 5.25 (s, 2H, CH_2), 3.79 (s, 3H, OMe), 1.70 (s, 6H, CH_3). ^{13}C NMR (100 MHz, $CDCl_3$): δ 186.59 (CHO), 184.74 (C-N), 159.54, 145.13, 134.51, 133.19, 129.36, 128.80, 127.28, 115.66, 113.29, 109.90, 108.50, 55.92, 54.66, 53.87, 24.86. FT-IR (ATR): 3028,

2960, 2922, 2756, 1600, 1474, 1444, 1402, 1300, 1184, 1117, 1025, 808, 777, 704, 543 cm-1. HRMS (ESI): *m/z* $[M+H]^+$ calcd $C_{21}H_{22}NO_3$: 336.1594; found: 336.1598.

Compound 15: Brown solid. Yield: 9%. m.p = 176 – 177 °C. ^{1}H NMR (400 MHz, $CDCl_3$): δ 9.63 (s, 2H, CHO), 8.12 (d, 1H, *J* = 8.8 Hz, Ar-H), 7.88 (d, 1H, *J* = 8.4 Hz, Ar-H), 7.74 (d, 1H, *J* = 8.8 Hz, Ar-H), 7.63 (dt, 1H, *J* = 6.8, 1.2 Hz, Ar-H), 7.51 (dt, 1H, *J* = 8.0, 1.2 Hz, Ar-H), 7.29 (m, 4H, *J* = 8.4, 2.4 Hz, Ar-H), 7.17 (d, 1H, *J* = 1.6 Hz, Ar-H), 7.15 (s, 1H, Ar-H) 5.37 (s, 2H, CH_2), 2.04 (s, 6H, CH_3). ^{13}C NMR (100 MHz, $CDCl_3$): δ 188.00 (CHO), 186.50 (C-N), 138.53, 136.84, 134.03, 132.48, 129.93, 129.69, 129.25, 128.57, 127.78, 127.72, 127.18, 125.98, 122.92, 113.08, 110.23, 54.96, 54.69, 24.31. FT-IR (ATR): 2983, 2767, 1610, 1598, 1447, 1423, 1407, 1200, 1173, 933, 817, 781, 755 cm^{-1}. HRMS (ESI): *m/z* $[M+H]^+$ calcd $C_{24}H_{22}NO_2$: 356.1650; found: 356.1663.

General procedure for the preparation of zwitterions 16 – 25.

A solution of *N*-alkylated diformyl **6** – **15** (1 equiv.) and BA (1.1 equiv.) dissolved in a minimum amount of MeOH was refluxed for 3-4 h. Upon completion of the reaction as indicated by TLC, the solvent was evaporated to half of the initial volume under reduced pressure, the precipitate was collected, washed with 30% MeOH (aq) and dried at 60 °C to afford the pure product.

Zwitterion 16: Yellow solid. Yield: 74%. m.p = 291 – 292 °C. ^{1}H NMR (400 MHz, DMSO): δ 10.39 (s, 1H, N-H), 10.19 (s, 1H, N-H), 9.24 (s, 1H, CHO), 8.02 (s, 1H, olefin), 7.80 (d, 1H, *J* = 7.6 Hz, Ar-H), 7.70 (dd, 1H, *J* = 6.8, 0.8 Hz, Ar-H), 7.57 (m, 2H, *J* = 7.2, 1.2 Hz, Ar-H), 3.63 (s, 3H, CH_3), 1.33 (s, 6H, CH_3). ^{13}C NMR (100 MHz, DMSO): δ 192.75 (C-1), 187.40 (CHO), 164.89 (C-2')*, 164.72 (C-2)*, 152.49 (C-4), 151.31 (C-3), 142.84, 142.26, 129.09, 129.04, 123.47, 115.29, 109.34 (C-5), 95.02 (C-6), 57.61, 35.83, 23.56 (C-7). FT-IR (ATR): 3166, 3010, 2814, 1714, 1650, 1621, 1532, 1432, 1408, 1396, 1178, 938, 765, 549, 525 cm^{-1}. HRMS (ESI): *m/z* $[M+H]^+$ calcd $C_{18}H_{18}N_3O_4$: 340.1292; found: 340.1292. *interchangeable.

Zwitterion 17: Orange solid. Yield: 38%. m.p = 300 – 301 °C . ^{1}H NMR (400 MHz, DMSO): δ 10.43 (s, 1H, N-H), 10.25 (s, 1H, N-H), 9.23 (s, 1H, CHO), 8.02 (s, 1H, olefin), 7.90 (d, 1H, *J* = 2.0 Hz, Ar-H), 7.83 (d, 1H, *J* = 8.4 Hz, Ar-H), 7.64 (dd, 1H, *J* = 8.8, 2.4 Hz, Ar-H), 3.60 (s, 3H, CH_3), 1.35 (s, 6H, CH_3). ^{13}C NMR (100 MHz, DMSO): δ 193.08 (C-1), 187.30 (CHO), 164.90 (C-2')*, 164.68 (C-2)*, 152.42 (C-4), 151.28 (C-3), 144.86, 141.09, 133.90, 129.12, 124.04, 116.92, 109.02 (C-5), 95.36 (C-6), 57.78, 36.03, 23.39 (C-7). FT-IR (ATR):

2990, 2820, 1700, 1669, 1627, 1539, 1449, 1428, 1396, 1179, 900, 785, 555, 528 cm-1. HRMS (ESI): *m/z* $[M+H]^+$ calcd $C_{18}H_{17}ClN_3O_4$: 374.0902; found: 374.0903. *interchangeable.

Zwitterion 18: Orange solid. Yield: 85%. m.p = 310 – 311 °C. ^{1}H NMR (400 MHz, DMSO): δ 10.36 (s, 1H, N-H), 10.16 (s, 1H, N-H), 9.21 (s, 1H, CHO), 7.99 (s, 1H, olefin), 7.72 (d, 1H, *J* = 8.8 Hz, Ar-H), 7.32 (d, 1H, *J* = 2.4 Hz, Ar-H), 7.08 (dd, 1H, *J* = 8.8, 2.4 Hz, Ar-H), 3.81 (s, 3H, OMe), 3.60 (s, 3H, CH_3), 1.31 (s, 6H, CH_3). ^{13}C NMR (100 MHz, DMSO): δ 190.44 (C-1), 187.71 (CHO), 164.85 (C-2')*, 164.79 (C-2)*, 160.65, 152.62 (C-4), 151.38 (C-3), 144.91, 135.60, 116.31, 114.35, 109.57 (C-5), 109.49, 94.68 (C-6), 57.46, 56.51, 35.84, 19.07 (C-7). FT-IR (ATR): 3160, 2986, 2815, 2698, 1701, 1655, 1632, 1536, 1446, 1422, 1394, 1286, 1180, 1054, 783, 546, 525. HRMS (ESI): *m/z* $[M+H]^+$ calcd $C_{19}H_{20}N_3O_5$: 370.1397; found: 370.1394. *interchangeable.

Zwitterion 19: Orange solid. Yield: 57%. m.p = 283 – 284 °C. ^{1}H NMR (400 MHz, DMSO): δ 10.48 (s, 1H, N-H), 10.30 (s, 1H, N-H), 9.27 (s, 1H, CHO), 8.25 (d, 1H, *J* = 1.6 Hz, Ar-H), 8.14 (dd, 1H, *J* = 8.0, 1.2 Hz, Ar-H), 8.06 (s, 1H, olefin), 7.90 (d, 1H, *J* = 8.0 Hz, Ar-H), 4.35 (q, 2H, CH_2), 3.61 (s, 3H, CH_3), 1.40 (s, 6H, CH_3), 1.33 (t, 3H, CH_3). ^{13}C NMR (100 MHz, DMSO): δ 194.39 (C-1), 187.14 (CHO), 165.59 (C=O ester), 164.87 (C-2')*, 164.59 (C-2)*, 152.28 (C-4), 151.24 (C-3), 145.74, 143.11, 130.65, 130.13, 124.11, 115.41, 109.11 (C-5), 96.02 (C-6), 61.80, 57.70, 36.10, 24.05 (C-7), 14.71. FT-IR (ATR): 3167, 2987, 2822, 1709, 1694, 1657, 1607, 1516, 1419, 1390, 1291, 1240, 1182, 1103, 1084, 768, 547, 524 cm^{-1}. HRMS (ESI): *m/z* $[M+H]^+$ calcd $C_{21}H_{22}N_3O_6$: 412.1503; found: 412.1499. *interchangeable.

Zwitterion 20: Orange solid. Yield: 23%. m.p = 279 – 280 °C. ^{1}H NMR (400 MHz, DMSO): δ 10.45 (s, 1H, N-H), 10.27 (s, 1H, N-H), 9.27 (s, 1H, CHO), 8.23 (d, 1H, *J* = 1.6 Hz, Ar-H), 8.13 (dd, 1H, *J* = 8.4, 1.6 Hz, Ar-H), 8.06 (s, 1H, olefin), 7.89 (d, 1H, *J* = 8.4 Hz, Ar-H), 3.62 (s, 3H, CH_3), 1.39 (s, 6H, CH_3). ^{13}C NMR (100 MHz, DMSO): δ 194.45 (C-1), 187.15 (CHO), 167.12 (C=O acid), 164.88 (C-2')*, 164.61 (C-2)*, 152.29 (C-4), 151.24 (C-3), 145.49, 143.01, 131.13, 130.72, 124.29, 115.27, 109.13 (C-5), 95.90 (C-6), 57.67, 36.08, 24.11 (C-7). FT-IR (ATR): 3184, 3103, 3032, 2782, 1717, 1700, 1634, 1619, 1604, 1512, 1427, 1394, 1209, 1180, 1087, 937, 770, 735, 549, 525 cm^{-1}. HRMS (ESI) *m/z* $[M+H]^+$ calcd $C_{19}H_{18}N_3O_6$: 384.1190; found: 384.1191. *interchangeable.

Zwitterion 21: Orange solid. Yield: 75%. m.p = 269 – 271 °C. ^{1}H NMR (400 MHz, DMSO): δ 10.38 (s, 1H, N-H), 10.11 (s, 1H, N-H), 9.29 (s, 1H, CHO), 8.24 (m, 2H, *J* = 5.6, 2.8 Hz,

Ar-H), 8.17 (d, 1H, *J* = 7.6 Hz, Ar-H), 8.09 (s, 1H, olefin), 8.02 (d, 1H, *J* = 8.8 Hz, Ar-H), 7.73 (td, 1H, *J* = 6.8, 0.8 Hz, Ar-H), 7.67 (t, 1H, *J* = 7.2 Hz, Ar-H), 3.77 (s, 3H, CH_3), 1.58 (s, 6H, CH_3). ^{13}C NMR (100 MHz, DMSO): *δ* 193.59 (C-1), 187.86 (CHO), 164.88 (C-2')*, 164.83 (C-2)*, 152.74 (C-4), 151.34 (C-3), 139.60, 137.77, 133.35, 130.76, 130.30, 128.77, 127.94, 127.32, 123.94, 113.68, 109.18 (C-5), 94.62 (C-6), 59.20, 36.23, 23.78 (C-7). FT-IR (ATR): 3166, 3011, 2801, 1716, 1622, 1520, 1429, 1385, 1358, 1178, 1081, 1001, 935, 843, 808, 778, 551, 533, 520 cm^{-1}. HRMS (ESI) *m*/*z* $[M+H]^+$ calcd $C_{22}H_{20}N_3O_4$: 390.1448; found: 390.1457. *interchangeable.

Zwitterion 22: Yellow solid. Yield: 64%. m.p = 258 - 259 °C. ^{1}H NMR (400 MHz, DMSO): *δ* 10.40 (s, 1H, N-H), 10.24 (s, 1H, N-H), 9.27 (s, 1H, CHO), 8.05 (s, 1H, olefin), 7.70 (d, 1H, *J* = 7.2 Hz, Ar-H), 7.53 (dd, 2H, *J* = 8.0, 2.0 Hz, Ar-H), 7.44 (t, 1H, Ar-H), 7.35 (m, 4H, *J* = 8.8, 1.2 Hz, Ar-H), 7.18 (d, 1H, *J* = 8.0 Hz, Ar-H), 5.32 (s, 2H, CH_2), 1.43 (s, 6H, CH_3). ^{13}C NMR (100 MHz, DMSO): *δ* 195.23 (C-1), 188.45 (CHO), 164.78 (C-2', C-2), 152.70 (C-4), 151.26 (C-3), 143.56, 141.49, 133.30, 129.19, 128.84, 128.80 (2C), 128.66, 123.58, 116.68, 108.76 (C-5), 94.72 (C-6), 58.20, 53.37, 24.53 (C-7). FT-IR (ATR): 3174, 2983, 2807, 1687, 1652, 1595, 1533, 1428, 1394, 1177, 1104, 932, 747, 548, 521 cm^{-1}. HRMS (ESI): *m*/*z* $[M+H]^+$ calcd $C_{24}H_{22}N_3O_4$: 416.1605; found: 416.1599. X-ray quality crystals were grown from a DMF solution.

Zwitterion 23: Orange solid. Yield: 98%. m.p = 268 – 270 °C. ^{1}H NMR (400 MHz, DMSO): *δ* 10.47 (s, 1H, N-H), 10.31 (s, 1H, N-H), 9.27 (s, 1H, CHO), 8.04 (s, 1H, olefin), 7.94 (d, 1H, *J* = 1.6 Hz, Ar-H), 7.51 (dd, 2H, *J* = 7.6, 2.0 Hz, Ar-H), 7.45 (dd, 1H, *J* = 8.4, 1.6 Hz, Ar-H), 7.34 (m, 3H, *J* = 7.2, 3.6 Hz, Ar-H), 7.17 (d, 1H, *J* = 8.8 Hz, Ar-H), 5.32 (s, 2H, CH_2), 1.44 (s, 6H, CH_3). ^{13}C NMR (100 MHz, DMSO): *δ* 195.27 (C-1), 188.33 (CHO), 164.81 (C-2')*, 164.71 (C-2)*, 152.63 (C-4), 151.24 (C-3), 145.59, 140.27, 133.71, 133.10, 129.24, 128.87, 128.78 (2C), 124.16, 118.12, 108.51 (C-5), 95.00 (C-6), 58.39, 53.34, 24.49 (C-7). FT-IR (ATR): 3167, 2981, 2808, 1702, 1615, 1524, 1428, 1399, 1177, 786, 551, 528 cm^{-1}. HRMS (ESI): *m*/*z* $[M+H]^+$ calcd $C_{24}H_{21}ClN_3O_4$: 450.1215; found: 450.1206. *interchangeable.

Zwitterion 24: Yellow solid. Yield: 52%. m.p = 299 – 300 °C ^{1}H NMR (400 MHz, DMSO): *δ* 10.40 (s, 1H, N-H), 10.23 (s, 1H, N-H), 9.26 (s, 1H, CHO), 8.03 (s, 1H, olefin), 7.54 (dd, 2H, *J* = 8.0, 1.6 Hz, Ar-H), 7.34 (m, 2H, *J* = 5.6, 3.2 Hz, Ar-H), 7.30 (s, 2H, Ar-H), 7.06 (d, 1H, *J* = 8.8 Hz, Ar-H), 6.88 (dd, 1H, *J* = 8.8, 2.4 Hz, Ar-H), 5.28 (s, 2H, CH_2), 3.76 (s, 3H,

OMe), 1.41 (s, 6H, CH_3). ^{13}C NMR (100 MHz, DMSO): δ 192.95 (C-1), 188.73 (CHO), 164.88 (C-2')*, 164.68 (C-2)*, 160.33, 152.82 (C-4), 151.33 (C-3), 145.70, 134.69, 133.33, 129.19 (2C), 128.79, 117.65, 114.17, 109.48, 108.91 (C-5), 94.42 (C-6), 58.02, 56.44, 53.40, 24.51 (C-7). FT-IR (ATR):, 2982, 2820, 1701, 1644, 1621, 1525, 1422, 1395, 1176, 1053, 786, 546, 523 cm^{-1}. HRMS (ESI): *m/z* $[M+H]^+$ calcd $C_{25}H_{24}N_3O_5$: 446.1712; found: 446.1692. *interchangeable.

Zwitterion 25: Orange solid. Yield: 76%. m.p = 216 – 218 ^oC. ^1H NMR (400 MHz, DMSO): δ 10.40 (s, 1H, N-H), 10.15 (s, 1H, N-H), 9.33 (s, 1H, CHO), 8.27 (d, 1H, J = 8.4 Hz, Ar-H), 8.12 (s, 1H, olefin), 8.07 (d, 1H, J = 8.0 Hz, Ar-H), 7.99 (d, 1H, J = 8.8 Hz, Ar-H), 7.71 (td, 1H, J = 7.2, 1.2 Hz, Ar-H), 7.65 (td, 1H, J = 8.8, 1.2 Hz, Ar-H), 7.56 (dd, 2H, J = 8.0, 1.6 Hz, Ar-H), 7.40 (d, 1H, J = 8.8 Hz, Ar-H), 7.34 (m, 3H, J = 7.2, 2.8 Hz, Ar-H), 5.47 (s, 2H, CH_2), 1.68 (s, 6H, CH_3). ^{13}C NMR (100 MHz, DMSO): δ 196.16 (C-1), 188.93 (CHO), 164.88 (C-2')*, 164.74 (C-2)*, 153.05 (C-4), 151.28 (C-3), 138.95, 138.74, 133.43, 133.03, 130.26, 130.16, 129.23 (2C), 128.77, 128.63, 127.97, 127.49, 123.96, 114.70, 108.48 (C-5), 94.38 (C-6), 59.76, 53.49, 24.32 (C-7). FT-IR (ATR): 2990, 2813, 1713, 1663, 1602, 1516, 1422, 1385, 1176, 778, 535 cm^{-1}. HRMS (ESI): *m/z* $[M+H]^+$ calcd $C_{28}H_{24}N_3O_4$: 466.1761; found: 466.1773. *interchangeable.

Conflicts of interest

The authors declare that there are no conflict of interest during the production and submission of the manuscript.

Acknowledgements

The authors wish to thank University Malaya through the grants of IIRG010B-2019 and ST011-2019. Sunway University Sdn. Bhd. acknowledges Grant No. STR-RCTR-RCCM-001-2019 for the support of this work.

References

1. G. Mohammadi Ziarani, F. Aleali and N. Lashgari, *RSC Adv.*, 2016, **6**, 50895-50922.
2. Archana, V. K. Srivastava and A. Kumar, *Bioorg. Med. Chem.*, 2004, **12**, 1257-1264.
3. P. Singh, M. Kaur and P. Verma, *Bioorg. Med. Chem. Lett.*, 2009, **19**, 3054-3058.
4. V. A. Dixit, P. C. Rathi, S. Bhagat, H. Gohlke, R. K. Petersen, K. Kristiansen, A. K. Chakraborti and P. V. Bharatam, *Eur. J. Med. Chem.*, 2016, **108**, 423-435.
5. W. Shi, S. Zhao, Y. Su, Y. Hui and Z. Xie, *New J. Chem.*, 2016, **40**, 7814-7820.
6. K. Li, Y. Zhang, B. Qiao, F. Tao, T. Li, Y. Ding, F. M. Raymo and Y. Cui, *RSC Adv.*, 2017, **7**, 30229-30241.
7. X. Zhang, Y. Yan, Y. Hang, J. Wang, J. Hua and H. Tian, *Chem. Commun.*, 2017, **53**, 5760-5763.
8. J. Du, X. Li, S. Ruan, Y. Li, F. Ren, Y. Cao, X. Wang, Y. Zhang, S. Wu and J. Li, *Analyst*, 2020, **145**, 636-642.
9. R. Prajapati, K. Kimura and L. Mishra, *Inorg. Chim. Acta*, 2009, **362**, 3219-3224.
10. A. Karmakar, A. Paul, K. T. Mahmudov, M. F. C. Guedes da Silva and A. J. L. Pombeiro, *New J. Chem.*, 2016, **40**, 1535-1546.
11. K. T. Mahmudov, M. N. Kopylovich, A. M. Maharramov, M. M. Kurbanova, A. V. Gurbanov and A. J. L. Pombeiro, *Coord. Chem. Rev.* , 2014, **265**, 1-37.
12. Y. W. Cao, X. D. Chai, T. J. Li, J. Smith and D. Li, *Chem. Commun.*, 1999, 1605-1606.
13. T. Gelbrich, D. Rossi, C. A. Häfele and U. J. Griesser, *CrystEngComm*, 2011, **13**, 5502-5509.
14. N. N. Pesyan, Y. Hosseini, A. Shokr and E. Şahin, *J. Chin. Chem. Soc.*, 2012, **59**, 1561-1566.
15. E.-Y. Xia, J. Sun, R. Yao and C.-G. Yan, *Tetrahedron*, 2010, **66**, 3569-3574.
16. Q.-F. Wang, L. Hui, H. Hou and C.-G. Yan, *J. Comb. Chem.*, 2010, **12**, 260-265.
17. H. Hou, Y. Zhang and C.-G. Yan, *Chem. Commun.*, 2012, **48**, 4492-4494.
18. V. A. Peshkov, A. A. Peshkov, O. P. Pereshivko, K. Van Hecke, L. L. Zamigaylo, E. V. Van der Eycken and N. Y. Gorobets, *ACS Comb. Sci.*, 2014, **16**, 535-542.
19. G. Jin, J. Sun and C.-G. Yan, *RSC Adv.*, 2016, **6**, 84379-84387.
20. T. Kolev, R. Bakalska, R. W. Seidel, H. Mayer-Figge, I. M. Oppel, M. Spiteller, W. S. Sheldrick and B. B. Koleva, *Tetrahedron: Asymmetry*, 2009, **20**, 327-334.

21. I. Yavari, A. Aminkhani and S. Arab-Salmanabadi, *Monatsh. Chem.*, 2012, **143**, 1195-1198.
22. Y.-D. Cai, T.-Y. Chen, X. Q. Chen and X. Bao, *Org. Lett.*, 2019, **21**, 7445-7449.
23. M. Bauer, A. Rollberg, A. Barth and S. Spange, *Eur. J. Org. Chem.*, 2008, **2008**, 4475-4481.
24. F. Karcı and F. Karcı, *Dyes Pigm.*, 2008, **77**, 451-456.
25. M. C. Rezende, P. Campodonico, E. Abuin and J. Kossanyi, *Spectrochim. Acta A: Mol. Biomol. Spectr.*, 2001, **57**, 1183-1190.
26. Y. Nagao, T. Sakai, K. Kozawa and T. Urano, *Dyes Pigm.*, 2007, **73**, 344-352.
27. H. Lee, M. Y. Berezin, K. Guo, J. Kao and S. Achilefu, *Org. Lett.*, 2009, **11**, 29-32.
28. O. S. Kolosova, S. V. Shishkina, V. Marks, G. Gellerman, I. V. Hovor, A. L. Tatarets, E. A. Terpetschnig and L. D. Patsenker, *Dyes Pigm.*, 2019, **163**, 318-329.
29. S. Khopkar and G. Shankarling, *Dyes Pigm.*, 2019, **170**, 107645.
30. M. Matsui, Y. Haishima, Y. Kubota, K. Funabiki, J. Jin, T. H. Kim and K. Manseki, *Dyes Pigm.*, 2017, **141**, 457-462.
31. Q. Xiao, S. Yang, R. Wang, Y. Zhang, H. Zhang, H. Zhou and Z. a. Li, *Dyes Pigm.*, 2018, **154**, 137-144.
32. S. So, H. Choi, H. Min Ko, C. Kim, S. Paek, N. Cho, K. Song, J. K. Lee and J. Ko, *Sol. Energy Mater. Sol. Cells*, 2012, **98**, 224-232.
33. A. Q. Ramle, H. Khaledi, A. H. Hashim, M. A. Mingsukang, A. K. Mohd Arof, H. M. Ali and W. J. Basirun, *Dyes Pigm.*, 2019, **164**, 112-118.
34. M. M. Baradarani, A. Afghan, F. Zebarjadi, K. Hasanzadeh and J. A. Joule, *J. Heterocycl. Chem.*, 2006, **43**, 1591-1595.
35. S. Seifert, A. Seifert, G. Brunklaus, K. Hofmann, T. Rüffer, H. Lang and S. Spange, *New J. Chem.*, 2012, **36**, 674-684.
36. W. A. Garadi, Y. E. Bakri, C.-H. Lai, S. Karthikeyan, L. E. Ghayati, J. T. Mague and E. M. Essassi, *ChemistrySelect*, 2020, **5**, 4601-4607.
37. A. Q. Ramle, A. Karakas, A. K. M. Arof, M. Karakaya, M. Taser, A. Gozutok, C. Chin Fei, N. M. Julkapli and W. J. Basirun, *J. Heterocycl. Chem.*, 2020, **57**, 3566-3573.
38. S. Harisha, J. Keshavayya, B. E. Kumara Swamy and C. C. Viswanath, *Dyes Pigm.*, 2017, **136**, 742-753.
39. M. R. Zamanloo, A. n. Shamkhali, M. Alizadeh, Y. Mansoori and G. Imanzadeh, *Dyes Pigm.* , 2012, **95**, 587-599.

40. D. Lauvergnat and P. C. Hiberty, *J. Am. Chem. Soc.*, 1997, **119**, 9478-9482.
41. C. A. Coulson, *J. Phys. Chem.*, 1952, **56**, 311-316.
42. J. A. Balam-Villarreal, B. J. López-Mayorga, D. Gallardo-Rosas, R. A. Toscano, M. P. Carreón-Castro, V. A. Basiuk, F. Cortés-Guzmán, J. G. López-Cortés and M. C. Ortega-Alfaro, *Org. Biomol. Chem.*, 2020, **18**, 1657-1670.
43. H. Zhang, Y. Cui, F. Tao, D. Zhang, Z. Xu and L. Guo, *Spectrochim. Acta A: Mol. Biomol. Spectr.*, 2019, **223**, 117320.
44. S. Sasaki, G. P. C. Drummen and G.-i. Konishi, *J. Mater. Chem. C*, 2016, **4**, 2731-2743.
45. B. Hosseinzadeh, A. Salimi Beni, A. Najafi Chermahini, R. Ghahary and A. Teimouri, *Synth. Met.*, 2015, **209**, 1-10.
46. G. Haberhauer, R. Gleiter and C. Burkhart, *Chem. Eur. J.*, 2016, **22**, 971-978.
47. C. Reichardt, *Chem. Rev.* , 1994, **94**, 2319-2358.
48. B. S. Jursic, D. M. Neumann, Z. Moore and E. D. Stevens, *J. Org. Chem.*, 2002, **67**, 2372-2374.
49. J. C. S. Costa, R. J. S. Taveira, C. F. R. A. C. Lima, A. Mendes and L. M. N. B. F. Santos, *Opt. Mater.*, 2016, **58**, 51-60.
50. P. Singh, A. Baheti and K. R. J. Thomas, *J. Org. Chem.*, 2011, **76**, 6134-6145.
51. E. L. Spitler, S. P. McClintock and M. M. Haley, *J. Org. Chem.*, 2007, **72**, 6692-6699.
52. Agilent Technologies, CrysAlis PRO Agilent Technologies, Santa Clara, CA, 2014.
53. G. M. Sheldrick, *Acta Crystallogr. Sect. A* 2008, **64**, 112-122.
54. G. M. Sheldrick, *Acta Crystallogr. Sect. C*, 2015, **71**, 3-8.
55. L. J. Farrugia, *J. Appl. Cryst.*, 2012, **45**, 849-854.
56. D. K. Brandenburg, DIAMOND, Crystal Impact GbR, Bonn (Germany) 2006.

Table of Contents

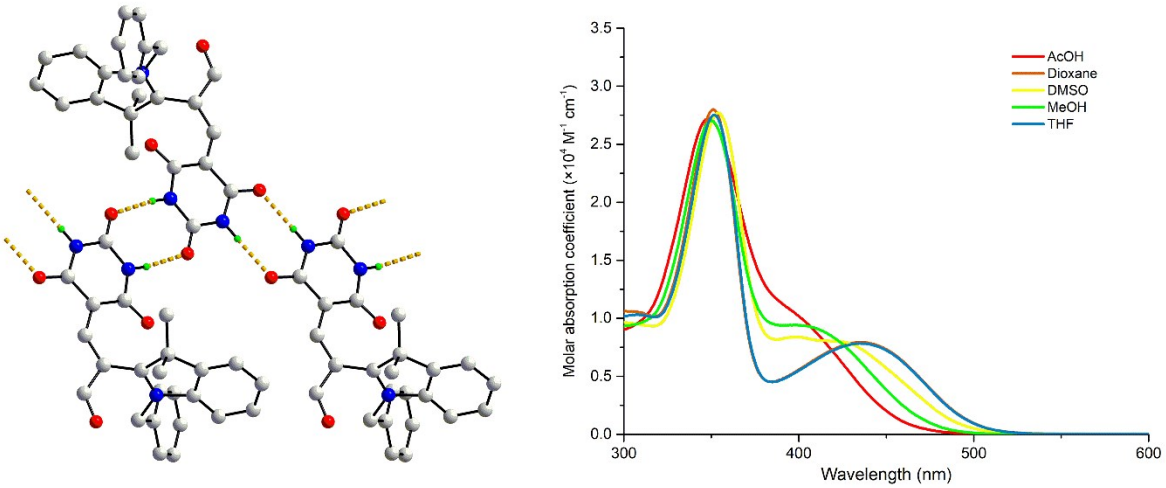

Graphical abstract

The intermolecular hydrogen bonding of barbiturates assists in the supramolecular aggregation and show a hypsochromic shift in protic solvents.